Polish Society of Composite Materials
Polskie Towarzystwo Materiałów Kompozytowych

24: 1 (2024) 49-56

COMPOSITES THEORY AND PRACTICE

ISSN (online): 2299-128X

Vipin Kumar Sharma[1], Pardeep Kumar[2]*, Dinesh Kumar[3], Rupesh Chalisgaonkar[4], Shalom Akhai[5]

[1] *IIMT University, Department of Mechanical Engineering, Meerut, U.P., 250005, India*
[2] *Maharishi Markandeshwar (Deemed to be University), Department of Mechanical Engineering, Ambala, India*
[3] *NIT Kurukshetra, Department of Mechanical Engineering, Haryana, India*
[4] *SRMIST Delhi NCR Campus, Department of Mechanical Engineering, Ghaziabad, U.P., India*
[5] *Chandigarh Group of Colleges, Department of Mechanical Engineering, Jhanjheri, Punjab, India*
**Corresponding author: E-mail: pardeepkamboj@yahoo.com*

Received (Otrzymano) 25.11.2023

CHARACTERIZATION OF Al 6061/Al_2O_3/SiC COMPOSITES WITH CERIUM OXIDE: CORROSION ANALYSIS AND MICROSTRUCTURAL INSIGHTS

https://doi.org/10.62753/ctp.2024.07.1.1

The aim of this research is to examine the corrosion characteristics of Al 6061/Al_2O_3/SiC composites when cerium oxide (CeO_2) is incorporated, employing electrochemical analysis and scanning electron microscopy (SEM) techniques. This study investigated the impact of cerium oxide on the corrosion behavior and assessed the hydrophobic properties of the composite surface in corrosive environments using contact angle measurements. The experimental methodology comprised several key components, like the selection of specific materials, the production of hybrid composites by the stir casting technique, the analysis of corrosion using the potentiodynamic polarization method, and the characterization of surface wettability. The metallographic analysis of the composites provided insights into the impact of various reinforcements on the microstructural properties. The incorporation of cerium oxide served to mitigate agglomeration and augment grain refinement within the composites. The utilization of potentiodynamic polarization analysis revealed enhanced corrosion resistance in hybrid composites containing cerium oxide in comparison to the Al 6061 alloy. The corrosion current density exhibited a decrease as the content of CeO_2 increased. The findings indicate that cerium oxide can effectively prevent corrosion in aluminum hybrid composites. These composites show potential for use in corrosion-prone applications.

Keywords: corrosion characteristics, Al 6061/Al_2O_3/SiC composites, cerium oxide (CeO_2), electrochemical analysis, scanning electron microscopy (SEM), surface wettability

INTRODUCTION

Over the last three decades, the production of engineering materials that are simultaneously lightweight, durable, and strong has emerged as a captivating subject of interest in both academic and industrial realms [1, 2]. Aluminum matrix composites (AMCs) have shown great potential in achieving these tailored properties due to their cost-effective construction, high strength-to-weight ratio, excellent castability, weldability, and wear properties [3, 4]. Nowadays, AMCs find applications in almost every field, from biomedical engineering to space exploration, as well as in defense applications and the automobile sector [5-7]. Hybrid AMCs have been fabricated using various types of reinforcing materials such as agricultural wastes, industrial by-products, and ceramic materials in powder form [8, 9]. Nevertheless, hybrid composites reinforced with ceramic materials have consistently been used in aerospace applications for performance optimization, with less emphasis on cost considerations. Among various ceramic synthetic particles, silicon carbide and alumina are primarily utilized [10, 11].

Literature reports indicate that over the past few years, a new category of ceramic reinforcement materials known as lanthanide series elements has gained significant traction in the realm of hybrid composites. These lanthanides, also referred to as rare earth elements (REE), are experiencing growing demand across various sectors owing to their exceptional properties [12, 13]. These properties include their hydrophobic nature, high strength, good thermal conductivity, magnetic attributes, excellent corrosion resistance, and thermal conductivity. Cerium, lanthanum, neodymium, and yttrium are prominent REEs that have been widely employed to enhance the mechanical properties of advanced matrix composites (AMCs). Zhang et al. [12] investigated the impact of an yttrium (Yb-70) addition on the microstructure and mechanical properties of 2519A aluminum alloy plates. These alloys find extensive use in the production of military aircraft, helicopters, drones, and various other potential mechanical applications. In their experiments, the researchers prepared three experimental alloys with weight percentages

(mass fractions) of Yb addition at 0.00%, 0.17%, and 0.30%, respectively. To examine the structure of the specimen, X-ray diffraction was employed using a D/Max 2500 X-ray diffractometer. Additionally, scanning electron microscopy (SEM) and transmission electron microscopy (TEM) were utilized to observe the microstructure of the prepared aluminum plates. Liu et al. [13] explored the influence of cerium oxide (CeO_2) on the microstructure and mechanical properties, including the hardness, tensile strength, and tensile elongation of the in situ titanium carbide/aluminum silicate (TiC/Al-Si) composite. In comparison to the TiC particle-reinforced composite, the Al-Si alloy exhibited greater weight loss. The incorporation of hard TiC particles into a relatively soft metallic matrix made of Al-Si contributed to a reduction in friction. Upon investigating the impact of the cerium oxide addition on the mechanical properties of the alloy, the researchers observed an increase in the hardness value (HB), tensile elongation, and tensile strength in comparison to the alloy without CeO_2.

Hydrophobic rare earth oxides (REOs) may enhance corrosion resistance in common cast aluminum alloys [14, 15]. Advanced matrix composites (AMCs) inhibit corrosion by forming a passive oxide layer [16]. The addition of a secondary phase in AMCs, however, leads to the splitting of oxide coatings, creating additional corrosion sites and accelerating composite deterioration. Consequently, corrosion studies have focused on hybrid composites with varied reinforcements. The hydrophobic nature, metal ion electrical topologies, and absence of polar contacts in REOs may impede electrochemical operations [17]. REOs derived from hydropower and marine sources exhibit corrosion resistance and hydrophobic properties, effectively resisting scaling and biofouling [18, 19]. The incorporation of REOs has been shown to enhance the durability of AMCs [20].

Researchers working on aluminum hybrid composites actively address corrosion issues, with hydrophobic secondary phases consistently demonstrated to reduce composite corrosion in numerous studies [21-23]. Rare earth coatings have proven effective in reducing the pitting corrosion of aluminum-based composites [24-26]. Corrosion-resistant properties were observed in Al 6092 composites with SiC when treated with cerium nitrate. Post-sulfuric acid anodization and cerium nitrate induced alterations in the composites led to improved composite corrosion resistance.

The present work focuses on the fabrication of hybrid composites reinforced with silicon carbides and alumina with traces amount of REEs. The aim of study is to investigate the influence of AMCs reinforced with various combinations of particles on the corrosion and hydrophobic properties. SEM examined how cerium oxide as an REE impacts the corrosion properties of Al 6061 AMCs. Finally, the hydrophobicity and corrosion resistance of the rare earth oxide composite surfaces in corrosive environments were tested.

MATERIALS AND METHODS

Materials

This study examined several matrix alloys and reinforcement combinations. The matrix material must be selected based on the application. The aim of the research is to develop an aluminum alloy-based composite that is both stable and non-reactive at the average working temperature for aviation materials. Table 1 shows the matrix, aluminum 6061 alloy.

TABLE 1. **Elemental composition in matrix alloy Al 6061**

Element	Mg	Si	Cu	Zn	Ti	Mn	Cr	Al
Composition [wt.%]	0.84	0.69	0.22	0.07	0.05	0.30	0.08	Balance

The material mechanical characteristics of the composite may be improved by selecting appropriate reinforcing materials. SiC, Al_2O_3, and CeO_2 are popular synthetic particles. Table 2 shows the morphology of the reinforcement used in the composites.

TABLE 2. **Morphological characteristics of various reinforcement particles**

Powder	Average particle length [µm]	Average particle width [µm]	Aspect ratio	Average particle size [µm]
SiC	55.7	29.5	1.89	39
Al_2O_3	50.5	28.3	1.78	42
CeO_2	29.7	9.9	2.99	16

Preparation of hybrid composites with SiC, Al_2O_3 and CeO_2

Bottom-pouring stir casting was utilized to produce Al 6061 alloy-SiC-Al_2O_3-CeO_2 hybrid composites. Different quantities of SiC, Al_2O_3, and CeO_2 were used in the process. The composites consisted of 2.5, 5, and 7.5 weight percent SiC and Al_2O_3. A small amount of CeO_2 (0.5-2.5%) was added as well. To ensure even distribution, the SiC and Al_2O_3 particles were mixed together, and packets containing 5, 10, and 15 wt.% of the mixture were prepared [27, 28].

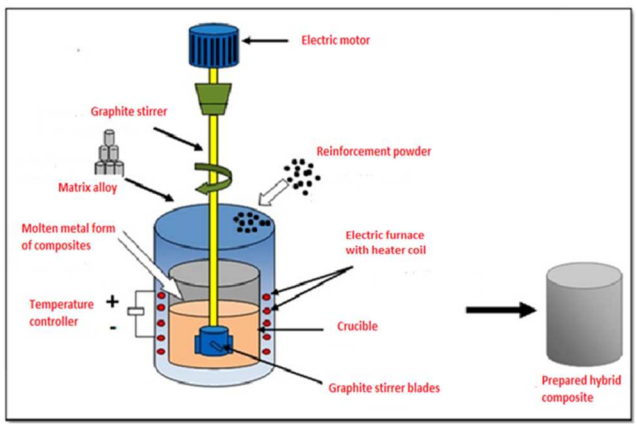

Fig. 1. Fabrication of aluminum hybrid composite via stir casting

These packets were then heated in an oven for 1 to 2 hours to oxidize their surfaces. The preparation process for Al_2O_3+SiC+CeO_2 followed a similar procedure. During manufacturing, a conical hopper was used to uniformly feed the warmed powder into the molten metal. A graphite stirrer was employed to mix the powder and molten metal for 8-10 minutes at 350 rpm. The hybrid composites were prepared by stir-casting method as shown in Figure 1.

Preparation of test specimens for corrosion testing via electrochemical technique

Using a potentiodynamic polarization electrochemical technique and a 3.5% NaCl solution at 300°C, the corrosion resistance of the hybrid composite samples was evaluated. The test specimens measured 20 mm by 30 mm. Each specimen featured a 1 mm^2 epoxy resin coating. The specimens were ground using sheets of 220-600 mesh silicon carbide abrasive. They were cleansed with deionized water and dried after being polished. The specimens were electropolished in a 20% perchloric acid/80% ethanol solution after being ground and polished. This enhanced the metallographic characterization of the specimen. SEM analysis was performed on the corroded specimens.

Evaluation of surface wettability using sessile drop analyzer

A sessile drop analyzer was used to perform wetting experiments on specimens of hybrid composites that measured 2 cm by 2 cm. The major components of the sessile drop analysis apparatus consisted of a quartz tube furnace, two vacuum pumps, and an image observation system. The hybrid composite specimens were horizontally aligned after being horizontally aligned on the graphite substrate. The quartz tube furnace was initially evacuated in order to achieve a vacuum pressure of 2.5 Pa at room temperature. After that, the furnace was warmed up to 1573 K. At regular intervals of 6 minutes, the contact angle was measured to assess the wetting qualities of the hybrid composites. Image processing software was utilized to assess the recorded images. The contact angles were measured on both sides to obtain an average.

RESULTS

Metallographic characterization

SEM was used to evaluate the interface effects between the reinforcing materials SiC, Al_2O_3, and CeO_2 of the produced composites. Figures 2a-f show hybrid composite microstructures with different reinforcement proportions at different magnifications. Figure 2a presents the dendritic silicon and alumina particles of the 2.5 wt.% SiC+Al_2O_3 hybrid composite. The composite cooling rate enhances the dendritic characteristics. The composite material solidifies with fewer dendrites when cooled properly. Figure 2b shows that reducing the size of the dendrites may improve the ductility of the composite material after casting. The spherical shape of SiC improves interparticle bonding and tensile strength. Kim et al. [29] found that a fine structure of Al_2O_3 particles increases the composite strength and matrix adherence, making the particle more difficult to remove. Figure 2c shows that hybrid composites with 7.5 wt.% SiC and Al_2O_3 have much finer Al_2O_3 particles than SiC particles. The Al_2O_3 particles are flaky and more difficult to remove than the SiC particles, which are spherical. Problems pulling out the particles may improve the hybrid composite tensile characteristics.

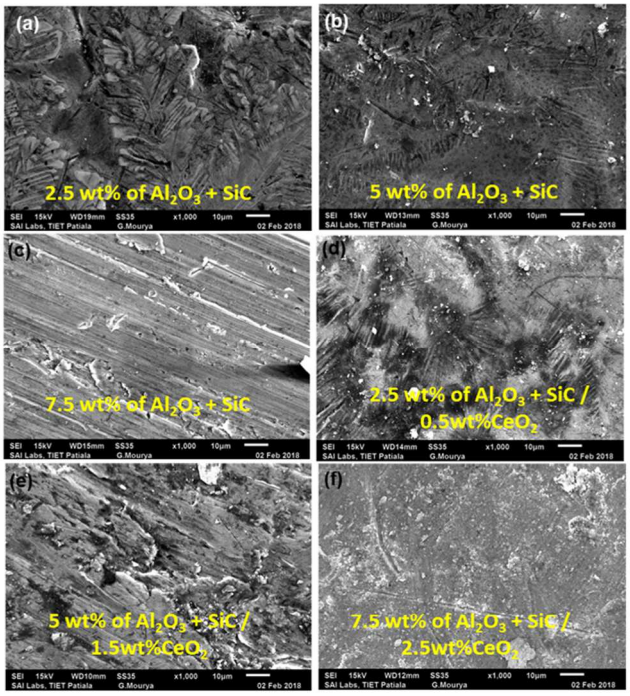

Fig. 2. SEM micrographs of hybrid composites with different reinforcement: a) 2.5 wt.% (SiC+Al_2O_3), b) 5 wt.% (SiC+Al_2O_3), c) 7.5 wt.% (SiC+Al_2O_3), d) 2.5 wt.% (SiC+Al_2O_3)+0.5 wt.% CeO_2, e) 5 wt.% (SiC+Al_2O_3)+1.5 wt.% CeO_2, f) 7.5 wt.% (SiC+Al_2O_3)+2.5 wt.% CeO_2

Rare earth oxides at 0.5-2.5 wt.% improve the mechanical characteristics. Figure 2d shows SEM micrographs with a visible decrease in CeO_2 particle aggregation. Reducing aggregation creates smoother composites. Xu and Ai [30] examined grain refinement in aluminum alloy A356 using europium (Eu) as a rare earth element. In 1999, Chong-hai et al. [31] demonstrated that europium improved the refining efficiency of aluminum alloys. Zheng and Yongmei [32] found that 0.5 wt.% yttrium gave aluminum alloy A356 a smooth and polished surface. Rare earth oxide reduces micro cuts and porosity, as seen in Figures 3e-f. The CeO_2 and aluminum oxide particles react to generate a homogenous phase. The cerium oxide particles refine the matrix grains as observed in the microstructural investigation of the composite, as seen in Figure 2f.

Chong-hai et al. [31] observed matrix grain refinement in aluminum alloys with europium additions.

Three phases dominate the hybrid composites with cerium oxide at weight percentages of 0.5, 1.5, and 2.5. EDS conducted at three points revealed three phases in the composite materials. The α-phase was found at Point 1, whereas at Point 2 it was the β-phase intermetallic complex and the ϒ-phase was present at Point 3. Matrix eutectic β-particles exhibit disclosed particle morphology. Rare earth oxides, particularly cerium dioxide (CeO_2), affect the composite properties. The cerium dioxide particles may be very small and acicular. EDS shows that the Al and Ce components of the ϒ-phase increase at Point 3.

Corrosion testing may be performed in three steps. Phase potential and micro-galvanic couples cause aluminum alloy corrosion. The β-phase of Al 6061 was cathodized. The β-phase of the Al 6061 alloy acts as a protective barrier and galvanic cathode, affecting corrosion. The β-phase protects the minute α-matrix particles when evenly dispersed. Rare earth compounds also reduce micro-galvanic corrosion from the α-phase anodic coupling of magnesium-based materials.

Potentiodynamic polarization measurement

The potentiodynamic polarization curves for the aluminum alloy and hybrid composites were examined to study the corrosion resistance of cerium oxide. The 2.5-3.5 weight percent sodium chloride solution had a potential of –1.5 V to 0.3 V.

The polarization curve of the Al 6061 alloy without rare earth oxides is not symmetrical and the anodic branch is steeper than the cathodic branch, indicating that the cathodic process has a greater impact on corrosion (Fig. 3a). Figure 3b-c shows the polarization curves of the hybrid composites with 0.5, 1.5, and 2.5 wt.% CeO_2. The corrosion potential shifts toward more noble values. The composites with CeO_2 had lower cathodic and anodic current densities than the Al 6061 alloy, indicating a controlled reaction. The polarization curve of aluminum alloy Al 6061 showed that the current density grows fast in the anodic zone with increasing potential, whereas the hybrid composites containing the rare earth oxide display a brief passive behavior.

Figure 3 presents the anodic and cathodic polarization of the Al 6061 alloy and hybrid composites with REO. Extrapolating the Tafel lines of each anodic and cathodic curve yielded the corrosion kinetics parameters (E_{corr}, β_A, β_C, I_{corr}).

Table 3 shows that the initial current density of Al 6061 was 9.490. The corrosion current density decreases from 0.5 to 2.5 wt.% CeO_2. The corrosion current densities were 4.980, 2.510, and 0.799 for 0.5, 1.5, and 2.5 wt.% CeO_2, respectively.

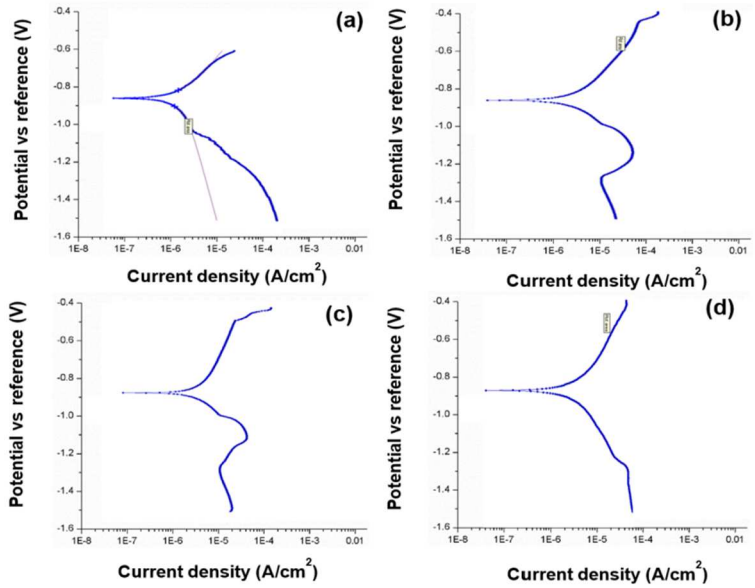

Fig 3. Polarization curves: a) Al 6061 alloys, b) hybrid composites with 0.5 wt.% CeO_2, c) hybrid composites with 1.5 wt.% CeO_2, d) hybrid composites with 2.5 wt.% CeO_2

TABLE 3. **Polarization curve results of Al 6061 alloy and hybrid composites with CeO_2**

Sample	Composition	Anodic Tafel constant β_A [mV/dec]	Cathodic Tafel constant β_C [mV/dec]	Corrosion current density I_{corr} [μA/cm²]	Corrosion potential E_{corr} [mV]	Corrosion rate [MPY]
1	Al6061	134.5	545.6	9.490	–945.0	3.512
2	Al6061/2.5 wt.%($SiC+Al_2O_3$)/0.5 wt.% CeO_2	38.20	577.5	4.980	–699.0	0.98
3	Al6061/5 wt.%($SiC+Al_2O_3$)/1.5 wt.% CeO_2	48.10	482.8	2.510	–712.0	0.27
4	Al6061/7.5 wt.%($SiC+Al_2O_3$)/2.5 wt.% CeO_2	82.50	274.5	0.799	–794.5	0.16

Role of cerium oxide as corrosion inhibitor

Morphology of alloy and composites using SEM

Figure 4 displays the surface morphologies of the corroded Al 6061 alloy and hybrid composites with the REO after 24 hours in 3.5 and 2.5 wt.% NaCl solutions. Figure 4a-b shows the Al 6061 corrosion, revealing thorough corrosion with a few cracks and pores. Pores and cracks allow chloride ions to enter the aluminum alloy and promote corrosion. The SEM micrographs in Figure 4c-f show that localized corrosion dominates the corrosion in the Al 6061 alloy composites as the cerium oxide content is increased from 0.5 wt.% to 2.5 wt.%. The micrographs show that just a portion of the surface is damaged and that the corrosion is greater on rough surfaces [33]. The other part of the surface shows a netlike structure and further corrosion phenomenon is inhibited. After adding white and acicular cerium oxide, the hybrid composite surface has plenty of Al and RE. The REO increased the Al 6061 alloy corrosion resistance by depressing micro-galvanic couplings between the α and β phases. Compared to β phases, α and phases have less potential [34]. The potentiodynamic polarization curves in Figure 4c-f reveal that homogenous REO dispersion in the Al 6061 alloy matrix may also increase hybrid composite corrosion resistance. It can also be observed from Figure 4c-f that the uniform dispersion of REO in the matrix of the Al 6061 alloy may be another factor in the improvement of the corrosion resistance of hybrid composites. Cerium oxide reduced localized corrosion. An Al-Mg matrix alloy reinforced with SiC exhibited comparable corrosion resistance trends [20]. Shimizu et al. [35] found that adding SiC to the Al-7075 matrix alloy increased the corrosion resistance by resisting stress caused by the NaCl solution.

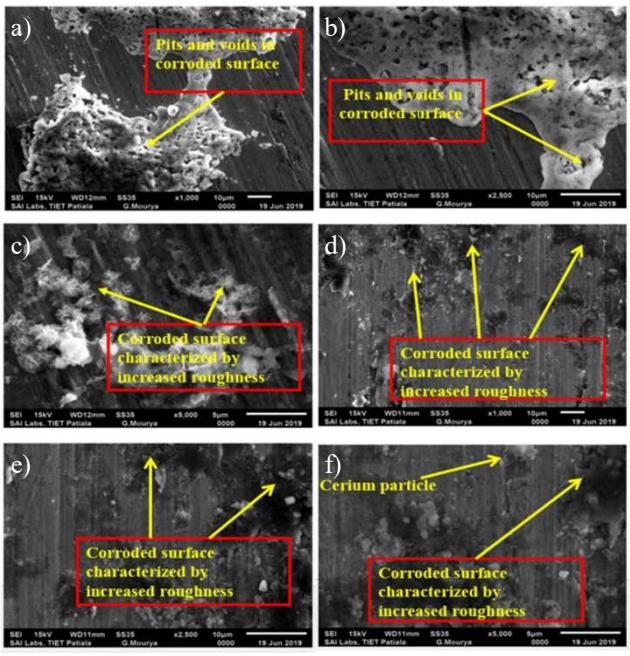

Fig. 4. Surface morphologies of corroded samples after 24 hours in 3.5 wt.% and 2.5 wt.% NaCl solution: a) Al 6061, b) Al 6061, c) 0.5 wt.% CeO_2, d) 1.5 wt.% CeO_2, e) 2.5 wt.% CeO_2, f) 2.5 wt.% CeO_2

Wettability analysis using contact angle approach

Relationship between wettability and corrosion resistance: Cassie-Baxter model

Wettability may be defined as the ability of a liquid to spread over a solid surface and represents the interaction between a liquid and a solid surface when in contact. Generally, wettability is described by the angle of contact made by the solid surface with a liquid drop. The concept of wettability at solid-liquid interfaces has been explored by various researchers using their own mathematical models based on important characteristics such as surface energy and contact angle. Currently, the most accurate mathematical model for determining the interaction energy between a liquid and a solid is the Thomas Young model.

In his model, Thomas Young employs the Laplace equation to establish the relationship between the contact angle and surface energy, providing a framework for defining wettability. Young uses Laplace equations to determine the shape of the droplet and the role of the contact angle under various boundary conditions, as illustrated in Figure 5. Before deriving the expression for the interaction energy between a liquid and a solid, the solid surface is assumed to be smooth, rigid, and homogeneous. In equilibrium conditions, the contact angle (θ) is defined by the Young-Dupré equation, as indicated in equation (1):

$$\gamma_{sv} = \gamma_{sl} + \gamma_{lv}\cos\theta \tag{1}$$

In equation (1), the terms γ_{sv}, γ_{sl} and γ_{lv} are related to the specific energy of the solid-vapor interface, specific energy of the solid-liquid interface, and specific energy of the liquid-vapor interface, respectively. Here, each specific energy or surface tension force can be understood as the tension force per unit area. As mentioned in Figure 5a, when a drop of liquid falls on a solid surface, such as a composite, it replaces a portion of the interface formed between the solid-vapor with a liquid-solid and liquid-vapor interface.

The phenomenon of liquid spreading will only occur if the above process results in a decrease in the free energy of the system under equilibrium conditions. The bonding force between the liquid and solid, i.e. the adhesion force (F_a), is defined as:

$$F_a = \gamma_{lv} + \gamma_{sv} - \gamma_{sl} \tag{2}$$

After combining both equation (1) and (2), we get

$$F_a = \gamma_{lv}(1 + \cos\theta) \tag{3}$$

It is evident that the bonding force between the liquid and solid phase can be expressed in terms of the contact angle (θ) and the surface tension of the liquid (γ_{lv}), as illustrated in Figure 5b-e. In Figure 5b, it is clear that for absolute wetting, $\theta = 0°$ and $\gamma_{sv} = = \gamma_{lv} + \gamma_{sl}$. Similarly, for good wetting, contact angle θ should lie between 0 and 90°. As the contact angle increases, the surface tension relation becomes

$\gamma_{sv} > \gamma_{sl}$ as indicated in Figure 5c. In Figure 5d, the contact angle falls between 90° and 180°, and due to the very large contact angle, $\gamma_{sv} < \gamma_{sl}$. A rise in the value of the surface energy at the solid-vapor interface compared to the solid-liquid interface indicates bad wetting. For non-wetting conditions, the contact angle should be 180°, and $\gamma_{sv} = \gamma_{lv} - \gamma_{sl}$, as seen in Figure 5e. Hence, the surface energy and contact angle measurements are the two factors defining the degree of wettability of a surface.

Building on the above discussions, the sessile drop analyzer method was generally employed to ascertain the wettability of the hybrid composites with SiC, Al_2O_3, and CeO_2. Six samples of the aluminum hybrid composites were prepared, with three samples reinforced with SiC and Al_2O_3 without the rare earth oxide, and three with the rare earth oxide, respectively. The probe liquid, usually water, was employed, considering the principle as stated by Thomas Young for determining the contact angle using the sessile drop method. After that, comparative analysis of the wettability of the hybrid composites was performed based on the contact angle. Our aim is generally to make the surface of hybrid composites hydrophobic, targeting aerospace body parts, including wings, structural components, and other accessories that are in direct contact with water.

The interaction between water and solids, in particular, can be classified as hydrophilic or hydrophobic, as shown in Figure 6. Materials that have an affinity for water are known as hydrophilic materials and cause water to spread across them, maximizing contact. Most materials tend to be hydrophilic, for example, metals usually spread water upon contact. Those that tend to repel water and cause water to bead up are known as hydrophobic materials. Generally, hydrophobic materials possess low surface energy and have a wide range of applications. Hydrophobic surfaces, in particular, have attracted significant attention over the past decade because of their broad technological potential. Considering this fact, the wettability of hydrophobic materials has been studied in the current work.

Figure 7 exhibits the hybrid composite contact angles with varying SiC, Al_2O_3, and CeO_2 fractions. The initial contact angle of the aluminum hybrid composites was 87.94°±1.58° when 2.5 wt.% SiC+Al_2O_3 was introduced. The composite surface will wet if the contact angle is less than 90 degrees. Surface dampness promotes corrosion [34]. In the hybrid composites with 2.5 wt.% SiC and Al_2O_3, adding 0.5 wt.% CeO_2 increases the contact angle to 99.07°±2.20°, exceeding 90° The surface is unfavorable for the wetting because of the increased contact angle. Thus, a condensed liquid droplet forms when the fluid reduces its surface contact. Compact droplets accumulate on the surface, reducing corrosion. A greater content of the rare earth oxide maintains compact droplet formation. A 5 wt.% combination of SiC and Al_2O_3 with 1.5 wt.% CeO_2 raised the contact angle from 96.72°±0.50° to 99.39°±1.14°. In the hybrid composites with 7.5 weight percent SiC and Al_2O_3, 2.5 weight percent CeO_2, the contact angle grows from 98.52 degrees with a standard deviation of 0.70 degrees to 100.78 degrees with an SD of 0.75 degrees. The higher REO content makes the aluminum hybrid composites hydrophobic, improving their corrosion resistance.

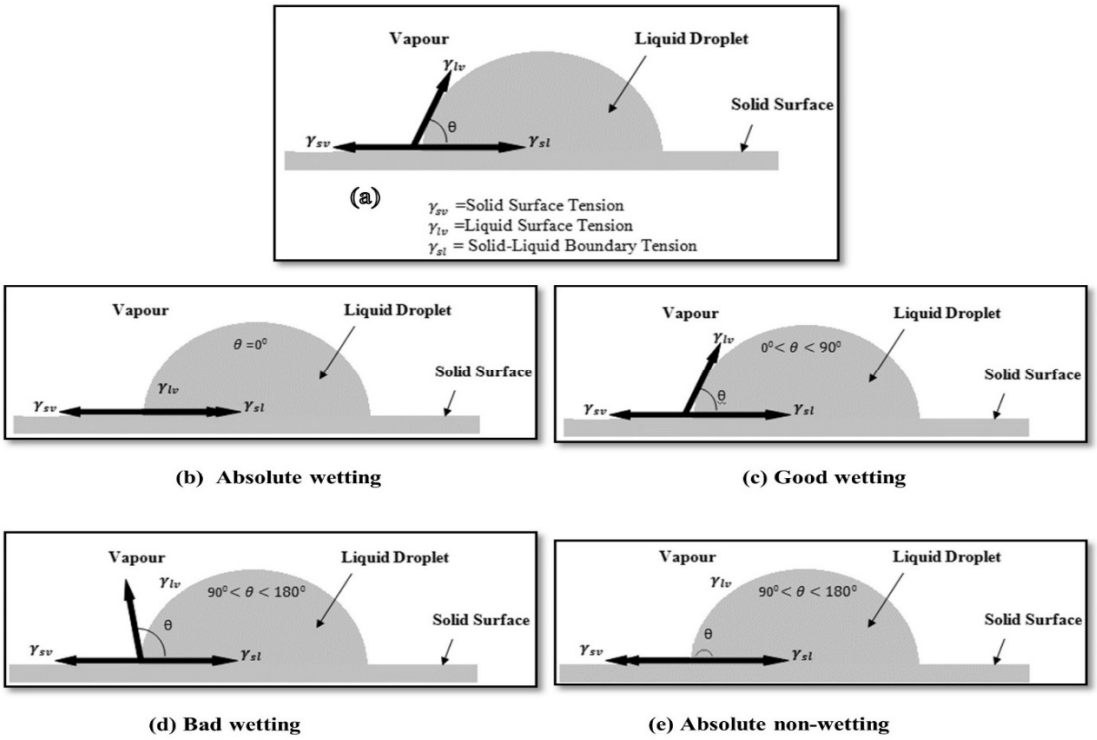

Fig. 5. Dependence of surface wettability on surface energy and contact angle (θ)

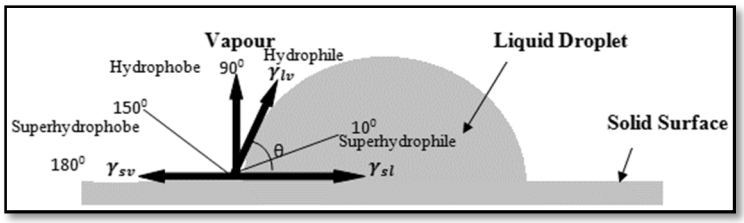

Fig. 6. Quantification of wetting properties in terms of contact angle (θ)

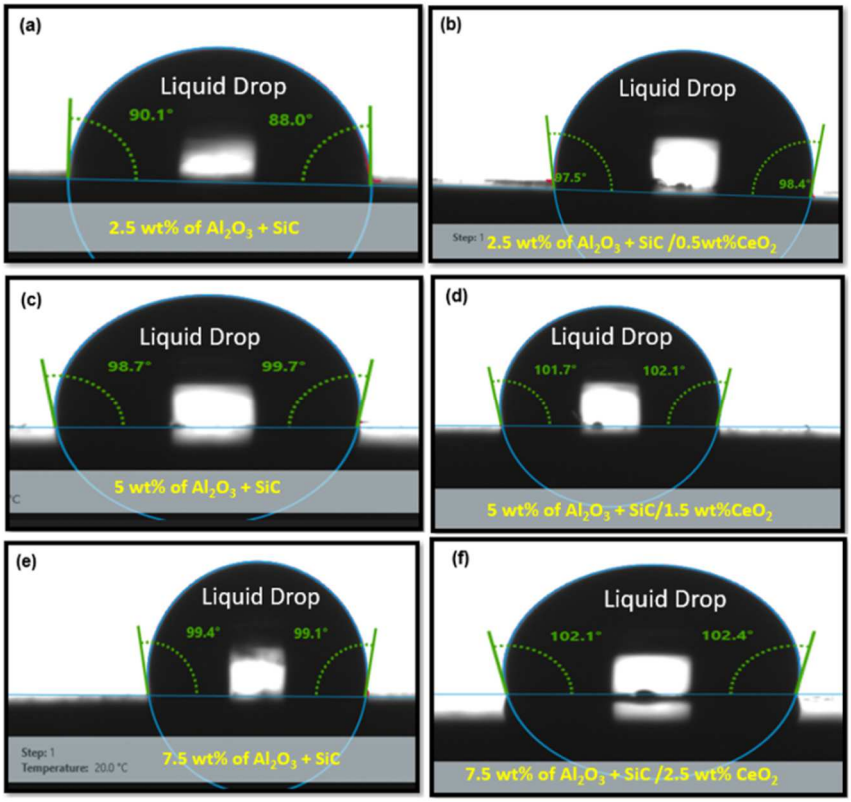

Fig. 7. Contact angle measurement for hybrid composites prepared via bottom pouring casting

CONCLUSIONS

This work investigated the corrosion characteristics of Al 6061/Al_2O_3/SiC composites with cerium oxide. Electrochemical analysis, SEM, and contact angle measurements assessed the corrosion and surface wettability. The empirical facts and analysis support the following conclusions:

– Cerium oxide improved the corrosion resistance in the Al 6061/Al_2O_3/SiC composites. The ideal cerium oxide concentration to reduce corrosion was 2.5 weight percent. As the cerium oxide concentration rose, the corrosion rates decreased, indicating that cerium oxide inhibits corrosion in the composites.
– Cerium oxide the refined the grains of the composite and reduced particle clustering. SEM examination revealed that cerium oxide improved the reinforcement particle dispersion and reduced particle agglomeration. The composites have an improved microstructure and corrosion resistance.
– The potentiodynamic polarization tests found that the hybrid composites with cerium oxide had better corrosion resistance than the Al 6061 alloy. As the cerium oxide concentration increased, the corrosion current density decreased, indicating that cerium oxide inhibits corrosion. SEM examination of the damaged composites revealed localized corrosion. Cerium oxide reduced corrosion and localized pitting, creating a more homogenous, protected surface.
– The contact angle measurements showed that cerium oxide increased the hydrophobicity of the composite surface. According to the Cassie-Baxter model, the composites with the greater cerium oxide concentration have larger contact angles, indicating better corrosion resistance. The hydrophobic surfaces prevented corrosion and protected the composite materials from corrosive conditions.

Thus, cerium oxide increased the corrosion resistance in the Al 6061/Al_2O_3/SiC composites. Cerium oxide reduced agglomeration, refined the grains, and homogenized the composite microstructures. Cerium oxide inhibited localized corrosion and made the composite surface hydrophobic. For corrosion-prone applications, cerium oxide may be added to composites.

REFERENCES

[1] Thirumoorthy A., Arjunan T.V., Kumar K.S., Latest research development in aluminum matrix with particle reinforcement composites – a review, Materials Today: Proceedings 2018, 5(1), 1657-1665.

[2] Wang L., Tang S., High-performance fiber-reinforced composites: latest advances and prospects, Buildings 2023, 13(4), 1094.

[3] Sharma V.K., Kumar V., Joshi R.S., Effect of RE addition on wear behavior of an Al-6061 based hybrid composite Wear, 2019, 426-427, 961-974.

[4] Kamboj A., Kumar S., Singh H., Fabrication and characterization of Al6063/SiC composites, Proceedings of the Institution of Mechanical Engineers, Part B: Journal Engineering Manufacture 2013, 227(12), 1777-1787.

[5] Ikumapayi O.M., Ogedengbe T.S., Ogundipe A.T., Nnochiri E.S., Obende B.A., Afolalu S.A., Ceramics matrix composites for biomedical applications – a review, Materials Today: Proceedings 2023, DOI: 10.1016/j.matpr.2023.08.168.

[6] Kumar S., Sharma V.K., Kumar V., Joshi R.S., Jain S., Kumar P., A review of recent research on rare earth particle composite materials and structures with their applications, Transactions of the Indian Institute of Metals 2021, 74(11), 1-13.

[7] Sharma V.K., Kumar P., Akai S., Kumar V., Joshi R.S., Analyzing the tribological and mechanical performance of Al-6061 with rare earth oxides: An experimental analysis, Proceedings of the Institution of Mechanical Engineers, Part E: Journal of Process Mechanical Engineering 2023, 09544089231160003.

[8] Chandel R., Sharma N., Bansal S.A., A review on recent developments of aluminum-based hybrid composites for automotive applications, Emergent Materials 2021, 4(5), 1243-1257.

[9] Suresh N., Balamurugan L., Geethan K.A.V., Kumar M.S., Statistical analysis of mechanical properties of Al-SiC-WC and Al-SiC-Al_2O_3 hybrid composites, Materials Today: Proceedings 2021, 42, 312-318.

[10] Kumar P., Sharma V., Kumar D., Akhai S., Morphology and mechanical behavior of friction stirred aluminum surface composite reinforced with graphene, Evergreen 2023, 10(01), 105-110.

[11] Sharma V.K., Kumar V., Joshi R.S., Kumar A., Effect of REOs on tribological behavior of aluminum hybrid composites using ANN, In: Additive Manufacturing in Industry 4.0: Methods, Techniques, Modeling and Nano Aspects, CRC Press, 2022, 153-168.

[12] Zhang X.M., Wang W.T., Chen M.A., Gao Z.G., Jia Y.Z., Ye L.Y., Zheng D.W., Ling L.I.U., Kuang X.Y., Effects of Yb addition on microstructures and mechanical properties of 2519A aluminum alloy plate, Transactions of Nonferrous Metals Society of China 2010, 20(5), 727-731.

[13] Liu Y., Xu B., Li W., Cai X., Yang Z., The effect of rare earth CeO_2 on microstructure and properties of in situ TiC/Al-Si composite, Materials Letters 2004, 58(3-4), 432-436.

[14] Bai M., Kazi H., Zhang X., Liu J., Hussain T., Robust hydrophobic surfaces from suspension HVOF thermal sprayed rare-earth oxide ceramics coatings, Scientific Reports 2018, 8(1), 6973.

[15] Khan S., Azimi G., Yildiz B., Varanasi K.K., Role of surface oxygen-to-metal ratio on the wettability of rare-earth oxides, Applied Physics Letters 2015, 106(6).

[16] Kozhukharov S., Kozhukharov V., Schem M., Aslan M., Wittmar M., Wittmar A., Veith M., Protective ability of hybrid nano-composite coatings with cerium sulphate as inhibitor against corrosion of AA2024 aluminium alloy, Progress in Organic Coatings 2012, 73(1), 95-103.

[17] Azimi G., Dhiman R., Kwon H.M., Paxson A.T., Varanasi K.K., Hydrophobicity of rare-earth oxide ceramics, Nature Materials 2013, 12(4), 315-320.

[18] Pedraza F., Mahadik S.A., Bouchaud B., Synthesis of ceria based superhydrophobic coating on Ni20Cr substrate via cathodic electrodeposition, Physical Chemistry Chemical Physics 2015, 17(47), 31750-31757.

[19] Wadhwa A.S., Akhai S., Comparison of surface hardening techniques for En 353 steel grade, International Journal of Emerging Technology and Advanced Engineering 2014, 4(10), 194-203.

[20] Candan S., An investigation on corrosion behaviour of pressure infiltrated Al-Mg alloy/SiCp composites, Corrosion Science 2009, 51(6), 1392-1398.

[21] Bethencourt M., Botana F.J., Calvino J.J., Marcos M., Rodriguez-Chacon M.A., Lanthanide compounds as environmentally-friendly corrosion inhibitors of aluminium alloys: A review, Corrosion Science 1998, 40(11), 1803-1819.

[22] Twite R.L., Bierwagen G.P., Review of alternatives to chromate for corrosion protection of aluminum aerospace alloys, Progress in Organic Coatings 1998, 33(2), 91-100.

[23] Davó B., De Damborenea J.J., Use of rare earth salts as electrochemical corrosion inhibitors for an Al-Li-Cu (8090) alloy in 3.56% NaCl, Electrochimica Acta 2004, 49(27), 4957-4965.

[24] Chen C., Mansfeld F., Corrosion protection of an Al 6092/SiCP metal matrix composite, Corrosion Science 1997, 39(6), 1075-1082.

[25] Hamdy A.S., Beccaria A.M., Traverso P., Corrosion protection of aluminium metal-matrix composites by cerium conversion coatings, Surface and Interface Analysis 2002, 34(1), 171-175.

[26] Pardo A., Merino M.C., Arrabal R., Viejo F., Carboneras M., Munoz J.A., Influence of Ce surface treatments on corrosion behaviour of A3xx, x/SiCp composites in 3.5 wt.% NaCl, Corrosion Science 2006, 48(10), 3035-3048.

[27] Sharma V.K., Kumar V., Joshi R.S., Investigation of rare earth particle on tribological and mechanical properties of Al-6061 alloy composites for aerospace application, Journal of Materials Research and Technology 2019, 8(4), 3504-3516.

[28] Sharma V.K., Aggarwal D., Vinod K., Joshi R.S., Influence of rare earth particle on the mechanical & tribological properties of Al-6063/SiC hybrid composites, Particle Science and Technology 2021, 39(8), 928-943.

[29] Kim Y.W., Chun Y.S., Nishimura T., Mitomo M., Lee Y.H., High-temperature strength of silicon carbide ceramics sintered with rare-earth oxide and aluminum nitride, Acta Materialia 2007, 55(2), 727-736.

[30] Xu C., Ai X., Particle dispersed ceramic composite reinforced with rare earth additions, International Journal of Refractory Metals and Hard Materials 2001, 19(2), 85-88.

[31] Chong-hai X., Xing A., Chuan-zhen H., Jian-xin D., Jing-tian S., Microstructural characterization of toughening mechanisms of ceramic tool material with rare earth additive, Journal of Chinese Electron Microscopy Society 1999, 18(4), 443-449.

[32] Zheng L., Yongmei H., Effect of yttrium on the microstructure of a semi-solid A356 Al alloy, Rare Metals 2008, 27(5), 536-540.

[33] Sharma V.K., Kumar V., Joshi R.S., Manufacturing of stable hydrophobic surface on rare-earth oxides aluminium hybrid composite, Proceedings of the Institution of Mechanical Engineers, Part E: Journal of Process Mechanical Engineering 2021, 235(4), 899-912.

[34] Liu W., Cao F., Chang L., Zhang Z., Zhang J., Effect of rare earth element Ce and La on corrosion behavior of AM60 magnesium alloy, Corrosion Science 2009, 51(6), 1334-1343.

[35] Shimizu Y., Nishimura T., Matsushima I., Corrosion resistance of Al-based metal matrix composites, Materials Science and Engineering: A 1995, 198(1-2), 113-118.

